

Blind Signal Separation Methods for the Identification of Interstellar Carbonaceous Nanoparticles ^{*}

O. Berné^{1,2}, Y. Deville², and C. Joblin¹

¹ Centre d'Etude Spatiale des Rayonnements, CNRS et Université Paul Sabatier Toulouse 3, Observatoire Midi-Pyrénées, 9 Av. du Colonel Roche, 31028 Toulouse cedex 04, France,

`olivier.berne@cesr.fr`, `christine.joblin@cesr.fr`

² Laboratoire d'Astrophysique de Toulouse-Tarbes, CNRS et Université Paul Sabatier Toulouse 3, Observatoire Midi-Pyrénées, 14 Av. Edouard Belin, 31400 Toulouse, France,
`ydeville@ast.obs-mip.fr`

Abstract. The use of Blind Signal Separation methods (ICA and other approaches) for the analysis of astrophysical data remains quite unexplored. In this paper, we present a new approach for analyzing the infrared emission spectra of interstellar dust, obtained with NASA's Spitzer Space Telescope, using *FastICA* and Non-negative Matrix Factorization (NMF). Using these two methods, we were able to unveil the *source* spectra of three different types of carbonaceous nanoparticles present in interstellar space. These spectra can then constitute a basis for the interpretation of the mid-infrared emission spectra of interstellar dust in the Milky Way and nearby galaxies. We also show how to use these extracted spectra to derive the spatial distribution of these nanoparticles.

1 Introduction

The Spitzer Space Telescope (*Spitzer*) comprises one of today's best instruments to probe the mid-infrared (mid-IR) emission of interstellar dust in the Milky Way and nearby galaxies. This emission is mainly carried by very small (nanometric) interstellar dust particles. One of the goals of infrared astronomy is to identify the physical/chemical nature of these species, as they play a fundamental role in the evolution of galaxies. Unfortunately, the observed spectra are mixtures of the emission from various dust populations. The strategy presented in this paper is to apply Blind Signal Separation (BSS) methods i.e. *FastICA* and NMF to a set of *Spitzer* mid-IR (5-30 μm) spectra obtained with the InfraRed Spectrograph (IRS), in order to extract the genuine spectrum of each population of nanoparticles. We first present these observations in Sect. 2, then we apply the

^{*} This work is based on observations made with the Spitzer Space Telescope, which is operated by the Jet Propulsion Laboratory, California Institute of Technology under a contract with NASA.

two BSS methods to these observations and finally give an example of how the extracted spectra can be used to trace the evolution of dust, in the Milky Way and external galaxies.

2 Observations

We have observed with *Spitzer* nearby photo-dissociation regions (PDRs), which consist of a star illuminating the border of dense clouds of gas and dust. The physical conditions (UV field intensity and hardness, cloud density) strongly vary from a PDR to another as well as inside each PDR depending on the considered position. These variations are extremely useful to probe the nature of dust particles which are altered by the local physical conditions [1]. Therefore, we have observed 11 PDRs as part of the SPEC-PDR program using the IRS in "spectral mapping" mode. This mode enabled us to construct one dataset for each PDR. This dataset is a spectral cube, with two spatial dimensions and one spectral dimension (see Fig. 1). Each spectral cube is thus a 3-dimensional matrix $C(p_x, p_y, \lambda)$, which defines the variations of the recorded data with respect to the wavelength λ , for each considered position with coordinates (p_x, p_y) in the cube. The dimensions of these cubes are generally about 30×30 positions and 250 points in wavelength ranging between 5 and $30 \mu\text{m}$.

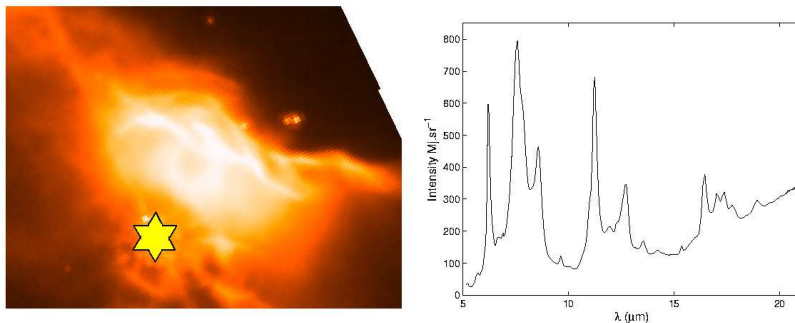


Fig. 1. *Left:* Infrared ($8 \mu\text{m}$) view of the NGC 7023 North PDR. The star is illuminating the cloud situated in the upper part of the image. *Right:* Mid-IR spectrum for a given position in the spectral cube of NGC 7023.

3 Blind Separation of Interstellar Dust Spectra

BSS is commonly used to restore a set of unknown "source" signals from a set of observed signals which are mixtures of these source signals, with unknown mixture parameters [2]. BSS is most often achieved using ICA methods such as *FastICA* [3]. An alternative class of methods for achieving BSS is NMF, which

was introduced in [4] and then extended by a few authors. In the astrophysical community, ICA has been successfully used for spectra discrimination in infrared spectro-imagery of Mars ices [5], elimination of artifacts in astronomical images [6] or extraction of cosmic microwave background signal in *Planck* simulated data [7]. To our knowledge, NMF has not yet been applied to astrophysical problems. However, it has been used to separate spectra in other application fields, e.g. for magnetic resonance chemical shift imaging of the human brain [8] or for analyzing wheat grain spectra [9].

The simplest version of the BSS problem concerns so-called "linear instantaneous" mixtures. It is modeled as follows:

$$X = AS \quad (1)$$

where X is an $m \times n$ matrix containing n samples of m observed signals, A is an $m \times r$ mixing matrix and S is an $r \times n$ matrix containing n samples of r source signals. The observed signal samples are considered to be linear combinations of the source signal samples (with the same sample index). It is assumed that $r \leq m$ in most investigations, including this paper. The objective of BSS algorithms is then to recover the source matrix S and/or the mixing matrix A from X , up to BSS indeterminacies.

The correspondence between the generic BSS data model (1) and the 3-dimensional spectral cube $C(p_x, p_y, \lambda)$ to be analyzed in the present paper may be defined as follows. In this paper, the sample index is associated to the wavelength λ , and each observed signal consists of the overall spectrum recorded for a cube pixel (p_x, p_y) . Each one of these signals defines a row of the matrix X in Eq. (1). Moreover, each observed spectrum is a linear combination of "source spectra" (see Sect. 3.1), which are respectively associated to each of the (unknown) types of nanoparticles that contribute to the recorded spectral cube. Therefore, the recorded spectra may here be expressed according to (1), with unknown combination coefficients in A , unknown source spectra in S and an unknown number r of source spectra.

3.1 Suitability of BSS Methods for the Analysis of *Spitzer*-IRS Cubes

In order to apply the NMF or *FastICA* to the IRS data cubes, it is necessary to make sure that the "linear instantaneous" mixture condition is fulfilled. Here we consider that each observed spectrum is a linear combination of "source spectra", which are due to the emission of different populations of dust nanoparticles. The main effect that can disturb the linearity of the model is radiative transfer as shown by [10], because of the non-linearity of the equations. In our case however, this effect is completely negligible because the emission spectra we observe come from the surface of clouds and are therefore not altered by radiative transfer.

3.2 Considered BSS Methods

In this section, we detail which particular BSS methods we have applied to the observed data.

IV

NMF We used NMF as presented in [11]. The matrix of observed spectra X is approximated using

$$WH, \tag{2}$$

where W and H are non-negative matrices, with the same dimensions as in (1). This approximation is optimized by adapting the matrices W and H using the algorithm of [11] in order to minimize the divergence between X and WH . We implemented the algorithm with Matlab. Convergence is reached after about 1000 iterations (which takes less than one minute with a 3.2 GHz processor). The value of r (number of "source" spectra) is not imposed by the NMF method. Our strategy for setting it so as to extract the sources was the following:

- Apply the algorithm to a given dataset, with the minimum number of assumed sources, i.e. $\hat{r} = 2$, providing 2 sources.
 - If the found solutions are physically coherent and linearly independent, we consider that at least $\hat{r} = 2$ sources can be extracted.
 - Else, we consider that the algorithm is not suited for analysis (this never occurred in our tests).

- Try the algorithm on the same dataset but with $\hat{r} = 3$ sources.
 - If the found solutions are physically coherent and linearly independent, we consider that at least $\hat{r} = 3$ sources can be extracted.
 - Else, we consider that only two sources can be extracted, extraction was over with $\hat{r} = 2$ and thus $r = 2$.

- Same as previous step but with $\hat{r} = 4$ sources.
 - If the found solutions are physically coherent and linearly independent, we consider that at least $\hat{r} = 4$ sources can be extracted.
 - Else we consider that only three sources can be extracted, extraction was over with $\hat{r} = 3$ and thus $r = 3$.

...

Physically incoherent spectra exhibit sparse peaks (spikes) which cannot be PDR gas lines. We found $r = 3$ for NGC 7023-NW and $r = 2$ for the other PDRs, implying that we could respectively extract 3 and 2 spectra from these data cubes.

FastICA We used *FastICA* in the deflation version [3] in which each source is extracted one after the other and subtracted from the observations until all sources are extracted. The advantage of this *FastICA* method is that it is not necessary to fix, before running the algorithm, the number r of sources that we want to extract, as it is for NMF. The extraction of the sources takes less than one minute using *FastICA* coded with Matlab, and with a 3.2 GHz processor.

3.3 Results

Using the BSS methods presented in this paper, we were able to extract up to three source spectra from the *Spitzer* observations. The number r of sources found in a given PDR is always the same with NMF and *FastICA*. The three extracted spectra in NGC 7023 North are presented in Fig. 2. Two of them exhibit the series of aromatic bands which have previously been attributed to Polycyclic Aromatic Hydrocarbons (PAHs, [12] and [13]). These two spectra show different band intensity ratios. One is the spectrum of neutral PAHs (PAH⁰) while the other is due to ionized PAHs (PAH⁺). The last spectrum exhibits a continuum and aromatic bands, which can be attributed to very small carbonaceous grains (VSGs), possibly PAH clusters [14].

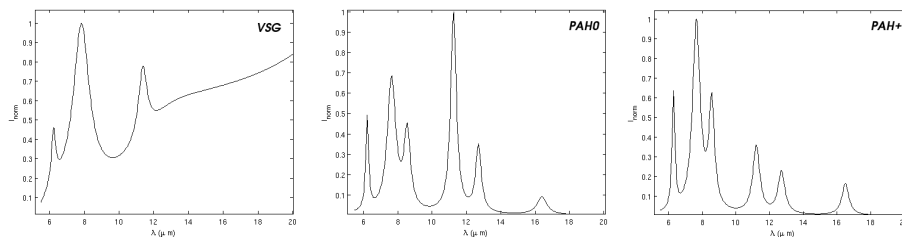


Fig. 2. The three BSS-extracted spectra from our study on PDRs.

3.4 *FastICA* vs NMF for our Application

As mentioned in Sect. 3.3, we were able to extract the source spectra from our data using both *FastICA* and NMF. However, the extracted spectra are not exactly the same for both methods. We conducted several tests in order to be able to evaluate which one of the two methods is more appropriate for our application. We created a set of 2/3 artificial carbonaceous nanoparticle spectra, to which we added a variable level of white, spatially homogeneous noise. We mixed these spectra with a random matrix to create a set of 100 artificial observed spectra. We then applied the two BSS methods considered in this paper. With a noise level at zero, both methods recover the original signals with high efficiency (correlation coefficients between original and extracted signals above 0.995). When adding noise, this efficiency decreases but remains acceptable down to a noise level corresponding to a SNR of 3dB (which is much lower than the average SNR of the *Spitzer spectra*). We note however that the efficiency of *FastICA* drops slightly faster than the one of NMF under the effect of an increasing noise, and drops dramatically below a SNR of 3dB, while NMF can still partly recover the original signals. Finally, with both methods we observe that the power of the residuals (i.e. observed signal minus signal reconstructed from the estimated sources and mixing coefficients) has the same level as *Spitzer* noise.

We have shown in Sect. 3.3 that there are two main populations: one with a continuum (VSGs) and one with bands only (PAHs). Using *FastICA*, we sometimes find a residual continuum in the BSS-extracted PAH spectrum, which we interpret as an incomplete separation. It is possible that the criterion of NMF is more appropriate in our case because less restrictive. Indeed, NMF only requires non-negativity of the sources and mixing coefficients, which is in essence the case for emission spectra, while *FastICA* is based on the statistical independence and non-gaussianity of the sources, which is more difficult to prove. As a conclusion, we would like to stress the fact that both methods are very efficient for the first task presented in this paper. We however note that NMF seems slightly better for this particular application.

4 Deriving the Spatial Distribution of Carbonaceous Nanoparticles

The next step of our analysis consists in using our extracted source spectra (Fig. 2) in order to determine the spatial distribution of the three populations in galactic clouds or in external galaxies. The *Spitzer* observations on-line archive contains hundreds of mid-IR spectral cubes of such regions which can be interpreted in this way. Our strategy consists in calculating the correlation parameter $c_p = E[Obs(p_x, p_y, \lambda)y_p(\lambda)]$ between an observed spectrum $Obs(p_x, p_y, \lambda)$ at a position (p_x, p_y) in a spectral cube and one of our extracted source spectra $y_p(\lambda)$, where $E[.]$ stands for expectation. With the considered (i.e. linear instantaneous) mixture model, each observed spectrum reads

$$Obs(p_x, p_y, \lambda) = \sum_n w(p_x, p_y)_n S_n(\lambda) \quad (3)$$

where $S_n(\lambda)$ is the n^{th} source spectrum and $w(p_x, p_y)_n$ are the mixing coefficients associated to that source. Moreover, BSS methods extract the sources up to arbitrary scale factors, i.e. they provide $y_p(\lambda) = \eta_p S_p(\lambda)$, where η_p is an unknown scale factor and $S_p(\lambda)$ is the p^{th} source. By centering the observations and thus the extracted spectra, and assuming that the sources are not correlated, the above-defined correlation parameter becomes

$$c_p = \eta_p w(p_x, p_y)_p E[S_p(\lambda)^2]. \quad (4)$$

This coefficient c_p is calculated for all the positions (p_x, p_y) , therefore yielding a 2D correlation map. Eq (4) shows that this map is proportional to $w(p_x, p_y)_p$ and thus defines the spatial distribution of the considered extracted source $y_p(\lambda) = \eta_p S_p(\lambda)$. We applied this approach to the spectral cube of NGC 7023 North (Fig. 1) and obtained the correlation maps presented in Fig. 3. We find that the three nanoparticle populations emit in very different regions. It appears from the maps of Fig 3 that there is an evolution from a population of VSGs to PAH⁰ and then PAH⁺ while approaching the star. This reveals the processing of the nanoparticles by the UV stellar radiation. The same strategy was tested

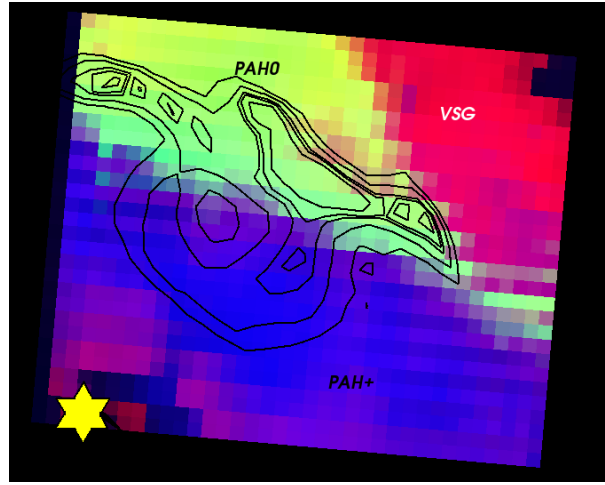


Fig. 3. Correlation maps of the three populations of nanoparticles in NGC 7023 North: VSGs in red, PAH^0 in green and PAH^+ in blue. The contours in black show the emission at $8 \mu m$ from Fig. 1. The slight correlation of VSGs with observations seen near the star is an artifact.

using the cubes of external galaxies from the *SINGS* program which provides a database of mid-IR spectral cubes for tens of nearby galaxies. Fig. 4 presents a map of the ratio of the two correlation parameters, resp. of PAH^0 and PAH^+ , obtained for the Evil Eye galaxy. This method provides a unique way to spatially trace the ionization fraction of PAHs which, combined with other tracers, is fundamental to understand the evolution of galaxies.

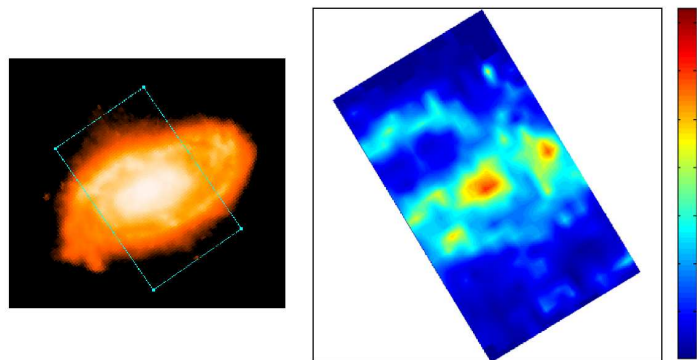


Fig. 4. *Left:* Infrared ($8 \mu m$) view of the NGC 4826 (Evil Eye) Galaxy. The rectangle indicates the region observed in spectral mapping with IRS. *Right:* Map of the ratio of PAH^0 over PAH^+ in NGC 4826 achieved using the BSS-extracted spectra (Fig.2).

5 Conclusion

Using two BSS methods, we were able to identify the genuine mid-IR spectra of three populations of carbonaceous nanoparticles in the interstellar medium. We have shown that both *FastICA* and NMF are efficient for this task, although NMF is found to be slightly more appropriate. The extracted spectra enable us to study the evolution of carbonaceous nanoparticles in the interstellar medium with unprecedented precision, including in external galaxies. These results stress the fact that BSS methods have much to reveal in the field of observational astrophysics. We are currently analyzing more spectral cubes observations from the *Spitzer* database using the strategy presented in this paper.

References

1. Rapacioli, M., Joblin, C., Boissel, P.: Spectroscopy of polycyclic aromatic hydrocarbons and very small grains in photodissociation regions. *Astronomy and Astrophysics* **429** (January 2005) 193–204
2. Hyvarinen, A., Karhunen, J., Oja, E. In Wiley, ed.: *Independent Component Analysis*. (2001)
3. Hyvarinen, A.: A Fast Robust Fixed Point Algorithm for Independent Component Analysis. *IEEE Transactions on Neural Networks* **10** (1999) 626–934
4. Lee, D.D., Seung, H.S.: Learning the parts of objects by non-negative matrix factorization. *Nature* **401** (October 1999) 788–791
5. Forni, O., Poulet, F., Bibring, J.P., The Omega Science Team: Component Separation of OMEGA Spectra with ICA. In: 36th Annual Lunar and Planetary Science Conference. (March 2005) 1623
6. Funaro, M., Erkki, O., Valpola, H.: Independent component analysis for artifact separation in astrophysical images. *Neural Networks* **16** (2003) 469–478
7. Maino, D., Farusi, A., Baccigalupi, C., Perrotta, F., Banday, A.J., Bedini, L., Burigana, C., De Zotti, G., Górski, K.M., Salerno, E.: All-sky astrophysical component separation with Fast Independent Component Analysis (FASTICA). **334** (July 2002) 53–68
8. Sajda, P., Du, S., Brown, T.R., Stoyanova, R., Shungu, D.C., Mao, X., Parra, L.C.: . *IEEE Transactions on Medical Imaging* **23** (December 2004) 1453–1465
9. Gobinet, A., Elhafid, A., Vrabie, V., Huez, R., Nuzillard, D. In: *Proceedings of the 13th European Signal processing Conference*. (Sep. 2005)
10. Nuzillard, D., Bijaoui, A.: Blind source separation and analysis of multispectral astronomical images. *Astronomy and Astrophysics, Supplement* **147** (November 2000) 129–138
11. Lee, D.D., Seung, H.S.: Algorithms for non-negative matrix factorization. In MIT press, ed.: *NIPS*. Volume 13. (2001) 556
12. Léger, A., Puget, J.L.: Identification of the 'unidentified' IR emission features of interstellar dust? *Astronomy and Astrophysics* **137** (August 1984) L5–L8
13. Allamandola, L.J., Tielens, A.G.G.M., Barker, J.R.: Polycyclic aromatic hydrocarbons and the unidentified infrared emission bands - Auto exhaust along the Milky Way. *The Astrophysical Journal, Letters* **290** (March 1985) L25–L28
14. Rapacioli, M., Calvo, F., Joblin, C., Parneix, P., Toubanc, D., Spiegelman, F.: Formation and destruction of polycyclic aromatic hydrocarbon clusters in the interstellar medium. *Astronomy and Astrophysics* **460** (December 2006) 519–531